Cofacial Assembly of Partially Oxidized Metallomacrocycles as an Approach to Controlling Lattice Architecture in Low-Dimensional Molecular Solids. Chemical and Architectural Properties of the "Face-to-Face" Polymers [M(phthalocyaninato)O]$_n$, Where M = Si, Ge, and Sn

Carl W. Dirk, Tamotsu Inabe, Karl F. Schoch, Jr., and Tobin J. Marks*

Contribution from the Department of Chemistry and the Materials Research Center, Northwestern University, Evanston, Illinois 60201. *Received June 7, 1982*

Abstract: This contribution reports a detailed chemical, spectroscopic, and X-ray diffractometric study of the nature and structures of the cofacially joined metallomacrocyclic polymers [M(Pc)O]$_n$, where M = Si, Ge, Sn and Pc = phthalocyaninato. These materials are precursors for a new class of electrically conductive polymers. Improved syntheses of the polymers are first reported. Optical spectra are assigned within the context of a porphyrinic "four orbital" model and related to those of the corresponding M(Pc)Cl$_2$ and M(Pc)(OH)$_2$ monomers. The vibrational spectra of the polymers are assigned, employing data from the aforementioned monomers and ^{18}O substitution. Identification of the M–O stretching modes allows an estimation of the polymer molecular weights as a function of polymerization procedure via an end group analysis. Degrees of polymerization obtained for typical samples are n = 120 (30) (M = Si), 70 (40) (M = Ge), 100 (40) (M = Sn). A parallel, radiotracer determination employing labeled M(Pc)(O^{3}H)$_2$ monomers yields results in favorable agreement. It is found that n can be substantially varied by controlling the polymerization conditions. X-ray diffraction measurements show the [M(Pc)O]$_n$ polymers to be highly crystalline. An analysis of the powder X-ray diffraction data has been carried out with carefully selected model compounds and computer simulation techniques. The results are in good accord with the proposed structure consisting of parallel chains of cofacially arrayed metallomacrocycles. The simplest structures which fit the experimental data are as follows: [Si(Pc)O]$_n$, orthorhombic space group *Ibam*, a = 13.80 (5) Å, b = 27.59 (5) Å, c = 6.66 (4) Å, Z = 4, interplanar spacing = 3.33 (2) Å, intrastack phthalocyanine staggering angle = 39 (3)°, density (g cm^{-3}) = 1.458 (21) (calcd), 1.432 (10) (found); [Ge(Pc)O]$_n$, tetragonal space group $P4/m$, a = 13.27 (5) Å, c = 3.53 (2) Å, Z = 1, interplanar spacing = 3.53 (2) Å, intrastack phthalocyanine staggering angle = 0 (5)°, density (g cm^{-3}) = 1.609 (28) (calcd), 1.512 (10) (found), or tetragonal space group $I4/m$, a = 18.76 (7) Å, c = 3.57 (2) Å, Z = 2, intrastack phthalocyanine staggering angle = 0 (5)°, density (g cm^{-3}) = 1.589 (26) (calcd), 1.512 (10) (found); [Sn(Pc)O]$_n$, tetragonal space group $P4/m$, a = 12.82 (5) Å, c = 3.82 (2) Å, Z = 1, intrastack phthalocyanine staggering angle ≈ 0°, density (g cm^{-3}) = 1.712 (25) (calcd), 1.719 (10) (found). The data for the latter structure are best fit to a model where the larger size of the Sn(IV) ion induces buckling of the macrocycle skeleton. An approximate analysis of the diffraction line widths suggests that crystallite dimensions are on the order of several hundred angstroms and are not grossly anisotropic.

Significant advances have recently been made in understanding the molecular and supermolecular characteristics which can imbue organic and metal–organic molecular solids with metal-like charge-transport, magnetic, and optical properties.[1] Two features are now recognized as necessary for transforming an unorganized collection of molecules into an electrically conductive array. First, the component molecules must be arranged in close spatial proximity and in crystallographically similar environments to provide a contiguous pathway for carrier delocalization. Second, the arrayed molecules must be in formal fractional oxidation states ("partial oxidation", "mixed valence", "incomplete charge transfer"); i.e., the molecular entities must have formally fractionally occupied valence shells. Within the framework of a simple, one-dimensional Hubbard description, this latter prerequisite is generally acknowledged to reflect the relatively narrow bandwidths ($4t$) and large on-site Coulomb repulsions (U) present in such materials.[1] The intense research activity in this area over the last few years has contributed considerably to the awareness of how these and other intra-/intermolecular parameters influence collective properties. Likewise, there has been a prodigious elaboration of the known classes of materials. Still, a general understanding of these materials in terms of the aforementioned parameters is at a very qualitative level. Furthermore, and of equal importance, the methodology to test ideas and to "tailor" new materials via rational chemical synthesis is presently at a rather primitive stage of evolution.

Initial activity in this Laboratory focused upon synthesizing and understanding the properties of new types of low-dimensional, mixed-valent solids containing metallomacrocyclic donor functionalities.[2] Thus, cocrystallization with halogens of conjugated, metal–ligand units having an MN$_4$ core structure (e.g., glyoximates (A, B),[2,3] phthalocyanines (C),[2,4] dibenzotetraazaannulenes (D),[2,5] hemiporphyrazines (E)[2,6,7]) results, in optimum cases, in segregated

(1) (a) Miller, J. S., Ed. "Extended Linear Chain Compounds"; Plenum Press: New York, 1982; Vol. 1, 2. (b) Alcácer, L., Ed. "The Physics and Chemistry of Low-Dimensional Solids"; D. Reidel: Dordrecht, 1980. (c) Devreese, J. T.; Evrard, V. E.; Van Doren, V. E., Eds. "Highly Conducting One-Dimensional Solids"; Plenum Press: New York, 1979. (d) Hatfield, W. E., Ed. "Molecular Metals"; Plenum Press: New York, 1979. (e) Torrance, J. B. *Acc. Chem. Res.* **1979**, *12*, 79. (f) Miller, J. S.; Epstein, A. J. *Ann. N.Y. Acad. Sci.* **1978**, *313*. (g) Keller, H. J., Ed. "Chemistry and Physics of One-Dimensional Metals"; Plenum Press: New York, 1977.

(2) Marks, T. J.; Kalina, D. W. in ref 1a; Vol. 1, pp 197–331.

(3) (a) Kalina, D. W.; Lyding, J. W.; Ratajack, M. T.; Kannewurf, C. R.; Marks, T. J. *J. Am. Chem. Soc.* **1980**, *102*, 7854–7862. (b) Cowie, M. A.; Gleizes, A.; Grynkewich, G. W.; Kalina, D. W.; McClure, M. S.; Scaringe, R. P.; Teitelbaum, R. C.; Ruby, S. L.; Ibers, J. A.; Kannewurf, C. R.; Marks, T. J. *Ibid.* **1979**, *101*, 2921–2936. (c) Brown, L. D.; Kalina, D. W.; McClure, M. S.; Ruby, S. L.; Schultz, S.; Ibers, J. A.; Kannewurf, C. R.; Marks, T. J. *Ibid.* **1979**, *101*, 2937–2947. (d) Gleizes, A.; Marks, T. J.; Ibers, J. A. *Ibid.* **1975**, *97*, 3545–3546.

(4) (a) Petersen, J. L.; Schramm, C. S.; Stojakovic, D. R.; Hoffman, B. M.; Marks, T. J. *J. Am. Chem. Soc.* **1977**, *99*, 286–288. (b) Schramm, C. S.; Scaringe, R. P.; Stojakovic, D. R.; Hoffman, B. M.; Ibers, J. A.; Marks, T. J. *Ibid.* **1980**, *102*, 6702–6713. (c) Stojakovic, D. R. Ph.D. Thesis, Northwestern University, 1978.

(5) (a) Lin, L.-S.; McClure, M. S.; Lyding, J. W.; Ratajack, M. T.; Wang, T.-C.; Kannewurf, C. R.; Marks, T. J. *J. Chem. Soc., Chem. Commun.* **1980**, 954–955. (b) Lin, L.-S.; McClure, M. S.; Lyding, J. W.; Ratajack, M. T.; Wang, T.-C.; Kannewurf, C. R.; Marks, T. J., submitted for publication.

(6) Dirk, C. W.; Stojakovic, D. R.; Marks, T. J., submitted for publication.

0002-7863/83/1505-1539$01.50/0

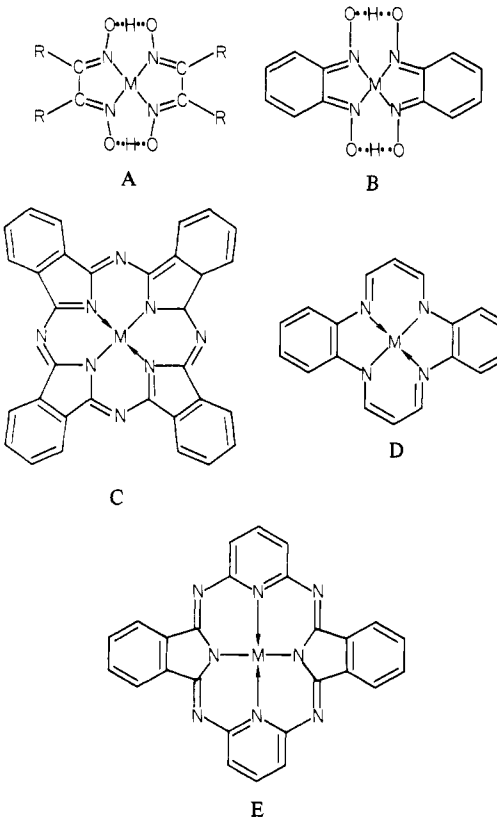

(DDD..., AAA...) arrays[3,8] of partially oxidized metallomacrocycles and halide or polyhalide counterions (eq 1). With resonance

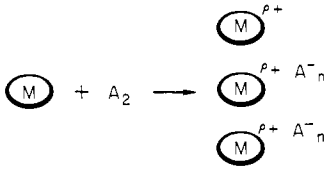

(1)

Raman and iodine Mössbauer techniques,[2,3,9] the form of the halogen (even if severely disordered) and thus the degree of incomplete charge transfer (ρ+) can be straightforwardly determined. A particularly successful example of this approach is the iodine oxidation of nickel phthalocyanine (C, M = Ni).[4] The product, $[Ni(Pc)]I_{1.0}$, crystallizes as stacks of staggered $Ni(Pc)^{0.33+}$ ligand-oxidized, π radical cations arrayed at 3.244 (2) Å separations and surrounded by columns of I_3^- counterions. In the stacking direction, the room temperature conductivity for typical crystals[4b,14b] is ca. 250–650 Ω^{-1} cm^{-1}, and the temperature dependence is "metal-like" ($d\sigma/dt < 0$), reaching a broad maximum (500–1500 Ω^{-1} cm^{-1}) by ca. 80 K, and then undergoing a smooth metal-to-semiconductor transition with $\sigma \lesssim 100$ Ω^{-1} cm^{-1} by 1.5 K.[14b] This behavior is reminiscent of highly conductive halogen-doped organic crystals such as TTT_2I_3.[2] The charge transport appears to be a largely ligand-centered process (e.g., $H_2(Pc)I_x$ materials are also highly conductive[4]) and carrier mean free paths are comparable to some of the most conductive "molecular metals".

Although the above and the other simple single molecule synthetic approaches to mixed-valent molecular materials are sometimes successful, they have severe limitations. They suffer from the weakness that the crystallization architecture is completely dependent upon the unpredictable and largely uncontrollable forces that dictate the stacking pattern, the donor–acceptor orientations, and the stacking repeat intervals. Even when such an approach is successful for a particular donor–acceptor combination, there is no guarantee that segregated stacking and other structural features will persist when modifications are made in either of the molecular components. Furthermore, for a given donor–acceptor pair, the structure is essentially "frozen" and little[10] can be done to modify intermolecular interactions. For these reasons, we have explored the possibility of controlling the stacking architecture in low-dimensional molecular solids by connecting charge-carrying molecular subunits through strong, covalent, structure-enforcing linkages.

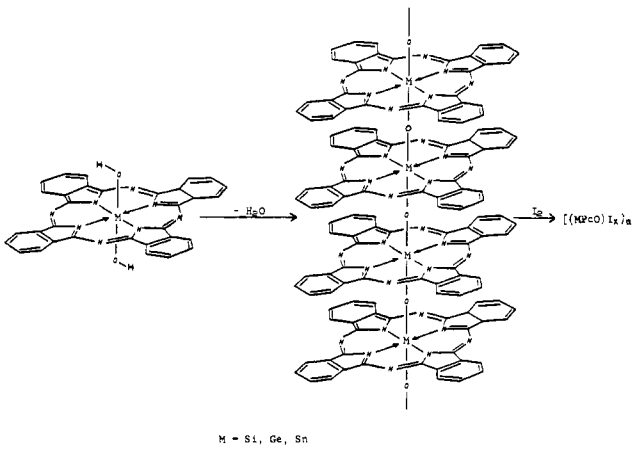

Figure 1. Scheme for the assembly and partial oxidation of a macromolecule composed of cofacially joined group 4A metallaphthalocyanine molecules.

We recently communicated[11] that the cofacial assembly of group 4A metallomacrocycles via condensation methodology originally pioneered by Kenney[12a] offers a viable means for rigorously enforcing donor stack architecture in low-dimensional mixed-valence materials. By the use of readily accessible, chemically flexible, well-characterized, robust subunits such as phthalocyanines[11,12b,c] (Figure 1), the approach builds upon existing molecular information and offers the possibility of delving into a number of the poorly understood features of the molecular "metallic" state. We showed that halogen doping of these materials led to a new and conceptually generalizable class[11c] of electrically conductive macromolecules, related both to single molecule systems as well as to electroactive polymers of great current interest.[13] In this

(7) For complementary studies with metalloporphyrins, see: Phillips, T. E.; Scaringe, R. P.; Hoffman, B. M.; Ibers, J. A. *J. Am. Chem. Soc.* **1980**, *102*, 3435–3444.

(8) For reviews of the structural chemistry of low-dimensional materials, see: (a) Grovers, H. A. J.; DeKruf, C. G. *Acta Crystallogr., Sect. A* **1980**, *A36*, 428–432 and references therein. (b) Keller, H. J. In ref 1b; pp 321–331. (c) Kistenmacher, T. J. In ref 1f; pp 333–342. (d) Metgert, S.; Pougent, J. P.; Comeš, R. In ref 1f; pp 234–243. (e) Stucky, G. D.; Schultz, A. J.; Williams, J. M. *Annu. Rev. Mater. Sci.* **1977**, *7*, 301–339. (f) Herbstein, F. H. *Perspect. Struct. Chem.* **1971**, *4*, 166–395.

(9) (a) Teitelbaum, R. C.; Ruby, S. L.; Marks, T. J. *J. Am. Chem. Soc.* **1980**, *102*, 3322–3328. (b) Teitelbaum, R. C.; Ruby, S. L.; Marks, T. J. *Ibid.* **1979**, *101*, 7568–7573.

(10) Variable-pressure studies represent a nonuniaxial approach. See, for example: (a) Jérome, D. In ref 1b; pp 123–142. (b) Metgert, S.; Comeš, R.; Pynn R.; Vettier, C.; Garito, A. F. In ref 1b; pp 101–112. (c) Webber, B.; Seiden, P. E.; Grant, P. M. *Phys. Rev. B: Condens. Matter* **1978**, *B18*, 2692–2700 and references therein.

(11) (a) Schoch, K. F., Jr.; Kundalkar, B. R.; Marks, T. J. *J. Am. Chem. Soc.* **1979**, *101*, 7071–7073. (b) Marks, T. J.; Schoch, K. F., Jr.; Kundalkar, B. *Synth. Met.* **1980**, 337–347. (c) Dirk, C. W.; Mintz, E. A.; Schoch, K. F., Jr.; Marks, T. J. *J. Macromol. Sci., Chem.* **1981**, *A16*, 275–298. (d) Marks, T. J.; Dirk, C. W.; Schoch, K. F., Jr.; Lyding, J. W. In "Molecular Electronic Devices", Carter, F. L., Ed.; Marcel Dekker: New York, 1982; pp 195–210.

(12) (a) Joyner, R. D.; Kenney, M. E. *J. Am. Chem. Soc.* **1960**, *82*, 5790–5791. (b) For investigations with isoelectronic group 3A $[M(Pc)F]_n$ systems, see: Nohr, R. S.; Kuznesof, P. M.; Wynne, K. J.; Kenney, M. E.; Siebenman, P. G. *Ibid.* **1981**, *103*, 4371–4377. (c) For results on similar $[M(Pc)L]_n$ materials where L is a bridging organic ligand and M is a transition metal, see: Schneider, O.; Hanack, M. *Mol. Cryst. Liq. Cryst.* **1982**, *81*, 273–284 and references therein; Diel, B. N.; Inabe, T.; Jaggi, N. K.; Lyding, J. W.; Schneider, O.; Hanack, M.; Kannewurf, C. R.; Marks, T. J.; Schwartz, L. H., submitted for publication.

(13) (a) Wynne, K. J.; Street, G. B. *Ind. Eng. Chem. Prod. Res. Dev.* **1982**, *21*, 23–28. (b) Baughman, R. H.; Brēdas, J. L.; Chance, R. R.; Elsenbaumer, R. L.; Shacklette, L. W. *Chem. Rev.* **1982**, *82*, 209–222. (c) Wegner, G. *Angew. Chem., Int. Ed. Engl.* **1981**, *20*, 361–381. (d) Duke, C. B.; Gibson, H. W. In "Kirk-Othmer Encyclopedia of Chemical Technology", 3rd ed.; Wiley: New York, 1982; Vol. 18, pp 755–793. (e) Seymour, R. B., Ed. "Conductive Polymers", *Polym. Sci. Technol.* **1981**, *16*.

and the accompanying contribution,[14a] we relate, in detail, our chemical and physical studies of halogen-doped $[M(Pc)O]_n$ systems, M = Si, Ge, Sn. We begin with an examination of the chemical and structural characteristics of the precursor macromolecules prior to doping. This includes new information on the syntheses, chemical reactions, spectroscopic properties, molecular weights, and crystal structures. We then explore structure, oxidation state, charge transport, and magnetic and optical properties in detail as a function of M and dopant level. It is seen that materials ranging from "molecular metals" to wide-gap semiconductors are achievable and that information of relevance both to molecular materials (e.g., the effects of varying the stacking repeat distance) and to conductive polymers (e.g., the homogeneity of the halogen doping) is derivable. Because stacking in the present systems is now enforced by strong covalent bonds rather than by weak packing forces, the limitations on effective dopants are considerably reduced. These results will be discussed in subsequent articles.[14b-d]

Experimental Section

Elemental analyses were preformed by H. Beck, Northwestern Analytical Services Laboratory, Microtech Laboratories, or by Galbraith Laboratories. The solvents quinoline and chloronaphthalene were vacuum-distilled from BaO; pyridine was distilled from BaO under nitrogen, $CHCl_3$ and CH_2Cl_2 from P_2O_5 under nitrogen, benzene and ether from NaK/benzophenone under nitrogen, and methanol from Mg under nitrogen. Practical grade *o*-phthalonitrile (Eastman) was dried under high vacuum. The reagent $SiCl_4$ (Alfa) was distilled under N_2 prior to use, and $GeCl_4$ (Aldrich) was used without further purification. Anhydrous $SnCl_2$ was prepared from $SnCl_2 \cdot 2H_2O$ (Baker) by the literature procedure.[15a]

Synthesis of 1,3-Diiminoisoindoline. 1,3-Diiminoisoindoline was prepared from *o*-phthalonitrile by a modification of the method of Kenney et al.[15b] The isolation of the product was modified by allowing the reaction mixture to stand overnight and then cooling it to −78 °C before filtering. The pale-green solid was then washed with ether and dried in a vacuum dessicator. The workup procedure was repeated twice, giving a total yield of ca. 50% (mp 192–196 °C dec (lit.[16] mp 196 °C dec)). In our hands, recrystallization from methanol/ether resulted in significant decomposition.

Synthesis of Si(Pc)Cl_2. (Phthalocyaninato)silicon dichloride was prepared by a modification of the literature procedure.[15b] Silicon tetrachloride (120 mL; 1.06 mol) was added under nitrogen to 1.2 L of dry quinoline in a 2-L three-necked flask. The solution was brought quickly to reflux. The 1,3-diiminoisoindoline (109.4 g; 0.75 mol) was added to the solution *only* when the temperature had reached 200 °C. The resulting solution was refluxed for 30 min and was then allowed to cool slowly without stirring. When the reaction mixture had cooled to 50 °C (ca. 2 h), it was diluted with approximately 300 mL of chloroform to facilitate the subsequent workup. The cooled, diluted mixture was then centrifuged in portions and the product washed with chloroform to yield 67.2 g of purple, crystalline material (70% yield). Yields as high as 80% have been obtained by this procedure. Cooling the reaction mixture slowly, without stirring, gave the product with the largest crystals. A purer product can be obtained by sublimation (420 °C (10^{-3} torr)), although some decomposition occurs.

Anal. Calcd for $C_{32}H_{16}N_8SiCl_2$: C, 62.85; H, 2.64; N, 18.32; Cl, 11.59. Found: C, 63.04; H, 2.52; N, 18.45; Cl, 11.63.

Synthesis of Si(Pc)$(OH)_2$. (Phthalocyaninato)silicon dihydroxide was prepared via the route of Davison and Wynne[17] by hydrolysis of finely powdered Si(Pc)Cl_2 with aqueous NaOH and pyridine.

Anal. Calcd for $C_{32}H_{18}N_8SiO_2$: C, 66.89; H, 3.16; N, 19.50; Cl, 0.00. Found: C, 67.03; H, 3.34; N, 19.36; Cl, 0.42.

Synthesis of $[Si(Pc)O]_n$. Thermal polymerization studies of Si(Pc)$(OH)_2$ were conducted under dynamic vacuum (10^{-3} torr) in a calibrated Lindberg "Hevi-Duty" Model 59344 tube furnace. As outlined in the Discussion section and Table III, detailed studies of the conditions were carried out, with the results being monitored by various spectroscopic, radiochemical, and diffraction techniques (vide infra). Typical conditions for $n \approx 50$–100 samples are 1–12 h heating at 440 °C (10^{-3} torr), yielding the poly(phthalocyaninatosiloxane) as a dark purple powder.[18]

Anal. Calcd for $C_{32}H_{16}N_8SiO$: C, 69.06; H, 2.90; N, 20.12; Cl, 0.00. Found: C, 69.53; H, 3.05; N, 20.13; Cl, 0.11.

Synthesis of Ge(Pc)Cl_2. (Phthalocyaninato)germanium dichloride was prepared by a modification of the method of Joyner and Kenney.[12a] Germanium tetrachloride (11 mL, 0.1 mol) was added under nitrogen to 100 mL of quinoline and was brought quickly to reflux. When the temperature of the solution reached 200 °C, 60 g (0.39 mol) of phthalonitrile was added to the mixture. The solution was next refluxed for 4 h and was then allowed to cool slowly to room temperature (ca. 2 h). The purple microcrystalline product was next filtered off, washed with DMF and ether, and dried in air. The overall yield was 29.32 g (50%).

Anal. Calcd for $C_{32}H_{16}N_8GeCl_2$: C, 58.59; H, 2.46; N, 17.08. Found: C, 58.62; H, 2.46; N, 16.85.

Synthesis of Ge(Pc)$(OH)_2$. Hydrolysis of (phthalocyaninato)germanium dichloride was conducted by the method of Joyner and Kenney[12a] with a solution of pyridine and aqueous NH_3.

Anal. Calcd for $C_{32}H_{18}N_8GeO_2$: C, 62.08; H, 2.93; N, 18.10. Found: C, 62.00; H, 2.97; N, 17.83.

Synthesis of $[Ge(Pc)O]_n$. Thermal polymerization studies of Ge(Pc)$(OH)_2$ were carried out and monitored as already described for Si(Pc)$(OH)_2$ (see also the Discussion section and Table III). Methodology for typical $n \approx 50$–100 samples involved heating for 10–48 h at 440 °C (10^{-3} torr).

Anal. Calcd for $C_{32}H_{16}N_8GeO$: C, 63.94; H, 2.68; N, 18.64. Found: C, 63.39; H, 2.33, N, 18.69.

Synthesis of Sn(Pc)Cl_2. (Phthalocyaninato)tin dichloride was prepared by a modification of the method described by Kroenke and Kenney.[19b] Anhydrous $SnCl_2$ (36 g, 0.20 mol) and 80 g (0.62 mol) of phthalonitrile were added to 1 L of 1-chloronaphthalene. The solution was brought to reflux over a period of 1 h and was allowed to reflux for 3 h. After slowly cooling to room temperature, the solution was filtered and the resulting solid washed with benzene in a Soxhlet extractor for 24 h. The yield of purple microcrystalline product was 108 g (96%).

Anal. Calcd for $C_{32}H_{16}N_8SnCl_2$: C, 54.79; H, 2.30; N, 16.00; Cl, 10.10. Found: C, 53.90; H, 2.39; N, 15.47; Cl, 10.57.

Synthesis of Sn(Pc)$(OH)_2$. (Phthalocyaninato)tin dichloride was hydrolyzed by mixing 12.60 g (0.0179 mol) of Sn(Pc)Cl_2, 2.75 g (0.069 mol) of NaOH, 65 mL of pyridine, and 250 mL of H_2O. The mixture was refluxed for 5 h and then allowed to cool slowly. The blue solid was filtered off, washed with water, and dried in a vacuum desiccator.

Anal. Calcd for $C_{32}H_{18}N_8SnO_2$: C, 57.78; H, 2.73; N, 16.84; Cl, 0.00; Sn, 17.84. Found: C, 57.08; H, 3.08; N, 16.34; Cl, 0.22; Sn, 18.48.

Synthesis of $[Sn(Pc)O]_n$. (Phthalocyaninato)tin dihydroxide was dehydrated by heating under dynamic vacuum (10^{-3} torr) in a tube furnace at 325 °C for 30 min.

Anal. Calcd for $C_{32}H_{16}N_8SnO$: C, 59.39; H, 2.49; N, 17.31; Sn, 18.34. Found: C, 56.56; H, 2.63; N, 17.24; Sn 19.99.

Synthesis and Polymerization of M(Pc)$(O^3H)_2$ Compounds. Samples of M(Pc)Cl_2 compounds (200–300-mg scale) were hydrolyzed in Schlenk ware under N_2 as per the methodology described above, using dry pyridine, ^3H_2O (0.17 mCi/mL), and NaO^3H. The tritiated water was obtained from New England Nuclear Corp. and was made alkaline by the addition of an appropriate amount of freshly cut sodium at 0 °C. The resulting M(Pc)$(O^3H)_2$ compounds were isolated by centrifugation, washed with several portions of ^3H_2O and dry pyridine, and dried overnight under high vacuum. Purity of these products was routinely monitored by infrared spectroscopy. Samples of the M(Pc)$(O^3H)_2$ materials were then polymerized under high vacuum in a tube furnace at various temperatures for varying lengths of time. Tritium contents of corresponding monomers and polymers were determined, in duplicate, by the Assay Laboratory of New England Nuclear Corp., using standard combustion techniques (burning to ^3H_2O and standard scintillation counting). When the magnitude of the polymer molecular weights became evident, labeled monomer samples were routinely diluted by grinding with unlabeled monomer so that monomer and polymer tritium contents (and activities) would be more closely comparable. Sample activities routinely exceeded those necessary for accurate counting[20] by a factor of at least 10^3.

(14) (a) Diel, B. N.; Inabe, T.; Lyding, J. W.; Schoch, K. F., Jr.; Kannewurf, C. R.; Marks, T. J. *J. Am. Chem. Soc.* **1983**, *105* (following paper in this issue). (b) Inabe, T.; Lyding, J. W.; Moguel, M. K.; Kannewurf, C. R.; Marks, T. J. *J. Mol. Cryst. Liq. Cryst.*, in press. (c) Inabe, T.; Lyding, J. W.; Moguel, M. K.; Marks, T. J. *J. Phys.*, in press. (d) Dirk, C. W.; Inabe, T.; Lyding, J. W.; Schoch, K. F., Jr.; Kannewurf, C. R.; Marks, T. J. *J. Polym. Sci., Polym. Chem. Ed.*, in press.

(15) (a) Stephen, H. *J. Chem. Soc.* **1930**, 2786–2787. (b) Lowery, M. K.; Starshak, A. J.; Esposito, J. N.; Krueger, P. C.; Kenney, M. E. *Inorg. Chem.* **1965**, *4*, 128.

(16) Elvidge, J. A.; Linstead, R. P. *J. Chem. Soc.* **1932**, 5000–5003.

(17) Davison, J. B.; Wynne, K. J. *Macromolecules* **1978**, *11*, 186–191.

(18) Joyner, R. D.; Kenney, M. E. *Inorg. Chem.* **1962**, *1*, 717–718.

(19) (a) Sutton, L. E. Ph.D. Thesis, Case Western Reserve University, 1966. (b) Kroenke, W. J.; Kenney, M. E. *Inorg. Chem.* **1964**, *3*, 251–254. (c) Kroenke, W. J. Ph.D. Thesis, Case Western Reserve University, 1963.

(20) Dr. E. Kobayashi (New England Nuclear), private communication.

Scheme I

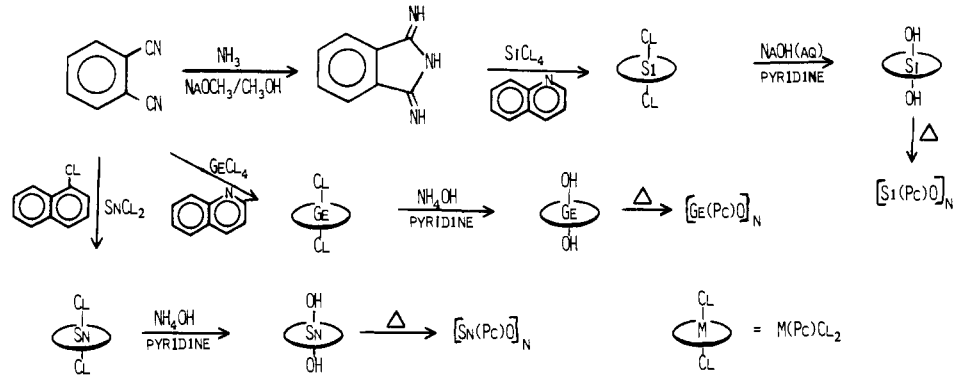

Synthesis and Polymerization of Si(Pc)(^{18}OH)$_2$. Freshly sublimed Si(Pc)Cl$_2$ (ca. 100 mg) was hydrolyzed in Schlenk ware as described above, using dry pyridine, $H_2{}^{18}O$ (Yeda Research and Development, >97% ^{18}O), and Na^{18}OH prepared by dissolving the appropriate amount of freshly cut sodium in $H_2{}^{18}O$ at 0 °C. The hydrolyzed product was collected by centrifugation, washed with pyridine, and dried under high vacuum. Polymerization was carried out at 440 °C for 1 h (10^{-3} torr).

Infrared Spectroscopy. Routine infrared spectra were recorded on Nujol mulls with Perkin-Elmer Model 283 or 599-B spectrometers and were calibrated with polystyrene film. Fourier transform spectra used for the end group analysis of the molecular weight or [Si(Pc)O]$_n$ materials were recorded on a Nicolet Model 7199 instrument. Four Fourier transform spectra were recorded for each sample of [Si(Pc)O]$_n$ investigated: background, KBr plates, KBr plates and Nujol, and KBr plates and Nujol mull of the sample. The spectra were collected with 0.5-cm^{-1} resolution (32 768 data points per scan) with 700 scans per spectrum, using a HgCdTe detector. After the interferograms were transformed and ratioed to the background spectrum, they were converted to spectra measured in absorbance. Next the spectrum of the KBr plates was subtracted from both the spectrum of the plates and Nujol as well as the spectrum of the sample. Then the Nujol spectrum was subtracted from the sample spectrum with the subtraction factor being determined by the disappearance of the Nujol absorptions at 1475 and 1365 cm^{-1} in the resultant spectrum. Estimation of the molecular weights of [Ge(Pc)O]$_n$ and [Sn(Pc)O]$_n$ was performed by using spectra recorded on the Perkin-Elmer 283 instrument. This subtraction technique required spectra with very high signal-to-noise ratios. The frequency range of interest for [Ge(Pc)O]$_n$ and [Sn(Pc)O]$_n$, 500–700 cm^{-1}, was found to be relatively noisy on the Fourier transform instrument due to noise from the detector and interference from atmospheric moisture and CO_2. For the Ge and Sn compounds, the Fourier transform instrument offered no advantages over the dispersive instrument in estimating the molecular weight. Results from three or more determinations were averaged for each calculation.

X-ray Diffraction. X-ray powder diffraction patterns of all compounds studied were recorded on a Rigaku Geigerflex recording powder diffractometer, using Ni-filtered Cu Kα radiation. The powders were pressed (8–10 tons on a ring press) into cylindrical pellets 13 mm in diameter and 1–2 mm thick. All patterns were recorded at a scanning rate of 0.25 deg min^{-1}. The apparatus was regularly calibrated by carefully recording the diffraction pattern of Si powder. The receiving slit was set at 0.6 mm and divergence and scattering slits set at 0.5° for $5° < 2\theta < 20°$, at 1° for $20° < 2\theta < 40°$, at 2° for $40° < 2\theta < 80°$, at 4° for $80° < 2\theta$ in order to expose the maximum sample area.

Samples were also pressed into rectangular tablets to assess the possible effects of preferential crystallite orientation[21a] on the diffraction patterns. Diffraction experiments were then conducted on "stacks" of these pellets, exposing either the "faces", which were in direct contact with the die face, or the "edges" (90° rotation of the tablet) to the X-ray beam. Comparison of the relative intensities of the various reflections within the patterns obtained in the two diffraction modes gave no evidence for preferential orientation—the patterns were identical.

Local versions of the computer programs INDX,[21b] POLSQ,[21c] and LAZY PULVERIX[21d] were employed for analyzing the [M(Pc)O]$_n$ powder diffraction data. The latter program generates theoretical powder patterns for different assumed crystal structures, while the former two can be used to iteratively fit observed data to certain assumed models. For derivation of crystal structure information, it was assumed that polymer metrical parameters were in accord with those of well-characterized (i.e., studied by single-crystal diffraction techniques) model compounds. These models included a variety of mononuclear phthalocyanine compounds,[22] the isoelectronic face-to-face gallium fluoride, [Ga(Pc)F]$_n$,[23a] [Ni(Pc)]$I_{1.0}$,[5b] Si(Pc)[OSi(CH$_3$)$_3$]$_2$,[23b] the face-to-face trimer [(CH$_3$)$_3$SiO]$_2$(CH$_3$)SiO-[Si(Pc)O]$_3$Si(CH$_3$)[OSi(CH$_3$)$_3$]$_2$,[23c] analogous group 4A porphyrin complexes,[24] and related group 4A R$_3$M–O–MR$_3$ compounds.[25] Thus, with the assumption of phthalocyanine internal dimensions in agreement with the model compounds (comparing metals of similar ionic radius[26]) and that the M–O–M axes were approximately linear and perpendicular to the macrocycle plane, theoretical patterns were generated (and compared visually with the experimental data) for unit cells of various symmetry, incrementally varying interplanar spacings (within reasonable limits of distances derived from the model compounds), angles of staggering between neighboring rings in a stack, the angle between the trans N–M–N axis and the unit cell edge, and interstack relationships. Great attention was devoted to avoiding convergence on a local minimum, and unrealistic nonbonded interactions were continuously checked with molecular models. Standard deviations were established by sequential variation of structural parameters once agreement between calculated and observed powder patterns had been reached.

Densities were measured by flotation in aqueous $ZnCl_2$ solutions.[27]

Optical Spectroscopy. Solution spectra of M(Pc)Cl$_2$ and M(Pc)(OH)$_2$ materials were recorded under N_2 in dry solvents, using matched cuvettes equipped with vacuum-tight Teflon needle valves. Solutions were prepared and transferred by using Schlenk/syringe or glovebox techniques. Spectra of solids were recorded as Nujol mulls between quartz plates. All spectra was recorded on a Perkin-Elmer Model 330 spectrophotometer. Multiple scans were routinely taken to verify that no decomposition or hydrolysis was occurring.

Results

Synthesis and Chemical Properties of M(Pc)Cl$_2$, M(Pc)(OH)$_2$, and [M(Pc)O]$_n$ Compounds. The poly(phthalocyaninatosiloxane), poly(germyloxane), and poly(stannyloxane) materials were pre-

(21) (a) Klug, H. P.; Alexander, L. E. "X-ray Diffraction Procedures for Polycrystalline and Amorphous Materials"; Wiley-Interscience: New York, 1974; Chapter 8. (b) Roof, R. B., Jr. "INDX: A Computer Program to Aid in the Indexing of X-Ray Powder Patterns of Crystal Structures of Unknown Symmetry", Los Alamos Scientific Laboratory, 1968, Report LA-3920. We thank Dr. Roof for the latest version of this program. (c) Cahen, D. Ph.D. Thesis, Northwestern University, 1974. We thank Professor J. A. Ibers for a copy of this program. (d) Yvon, K.; Jeitschks, W.; Parthé, E. *J. Appl. Crystallogr.* **1977**, *10*, 73–74. We thank D. Ketzsler for a local version of this program.

(22) (a) For compilations of structural data on M(Pc) complexes, see: Reference 5b. Day, V. W.; Marks, T. J.; Wachter, W. A. *J. Am. Chem. Soc* **1975**, *97*, 4519–4527. (b) Rogers, D.; Osborn, R. S. *J. Chem. Soc., Chem. Commun.* **1971**, 840 (Sn(Pc)Cl$_2$).

(23) (a) Nohr, R. S.; Wynne, K. J. *J. Chem. Soc., Chem. Commun.* **1981**, 1210–1211. (b) Mooney, J. R.; Choy, C. K.; Knox, K.; Kenney, M. E. *J. Am. Chem. Soc.* **1975**, *97*, 3033–3038. (c) Swift, D. R. Ph.D. Thesis, Case Western Reserve University, 1970.

(24) (a) Mavridis, A.; Tulinsky, A. *Inorg. Chem.* **1976**, *15*, 2723–2727 (Ge(porphyrinato)(OCH$_3$)$_2$). (b) Collins, D. M.; Scheidt, W. R.; Hoard, J. L. *J. Am. Chem. Soc.* **1972**, *94*, 6689–6696 (Sn(TPP)Cl$_2$). (c) Cullen, D. L.; Meyer, E. F., Jr. *Acta Crystallogr., Sect. B* **1973**, *B29*, 2507–2515 (Sn(OEP)Cl$_2$).

(25) (a) Glidewell, C.; Liles, D. C. *J. Organomet. Chem.* **1981**, *212*, 291–300 and references therein. (b) Glidewell, C.; Liles, D. C. *Ibid.* **1979**, *174*, 275–279 and references therein.

(26) Shannon, E. S. *Acta Crystallogr., Sect. A* **1976**, *A32*, 751–767.

(27) Tadokoro, H. "Structure of Crystalline Polymers"; Wiley-Interscience: New York, 1979; pp 82–83.

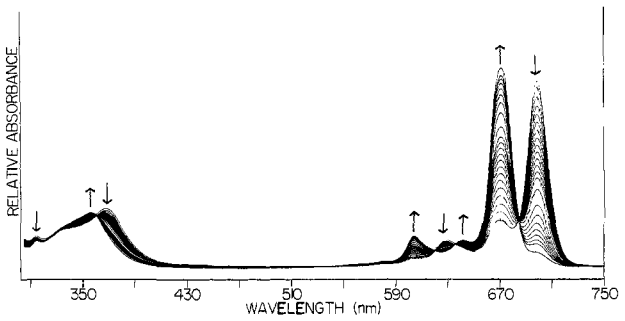

Figure 2. Spectrophotometric traces showing the result of exposing a solution of $Si(Pc)Cl_2$ in dry pyridine to air. Spectra were recorded over a period of 24 h.

pared via the routes outlined in Scheme I. This is basically the methodology of Kenney et al.,[11] but with some useful modifications. In the synthesis of $Si(Pc)Cl_2$, somewhat higher yields and appreciably purer products can be obtained if reflux times are held to a minimum (to avoid thermal decomposition of the quinoline solvent). In addition, thermal decomposition of the 1,3-diiminoisoindoline can be minimized if this reagent is not introduced until the $SiCl_4$/quinoline mixture has almost attained reflux. Experimentation established that the literature conditions[17] are essentially optimum for the hydrolysis of $Si(Pc)Cl_2$—longer reflux times result in decomposition. However, the moisture sensitivity of this complex in solution has not been previously appreciated. Thus, published[28] optical spectra are actually those of $Si(Pc)(OH)_2$ (vide infra), and hydrolysis is facile if rigorously anhydrous solvent and atmosphere are not maintained. A spectrophotometric illustration of this process is presented in Figure 2. Elemental analysis indicates that most $Si(Pc)(OH)_2$ samples contain traces of chloride.

Studies were conducted by monitoring the relative intensity of the 830-cm^{-1} Si–O stretch (vide infra) of $Si(Pc)(OH)_2$ in the infrared spectrum to establish optimum conditions for the thermal polymerization of $Si(Pc)(OH)_2$. $Si(Pc)(OH)_2$ is stable up to approximately 360 °C (in vacuo). Qualitatively, the dehydration begins slowly around 360 °C, requires ca. 40–50 min at 380 °C, and ca. 15 min at 400 °C. To ensure as complete polymerization as possible the reaction was routinely carried out at slightly higher temperature (440 °C) for longer periods of time (>1 h). Allowing the reaction to take place for 12 h at 440 °C did not significantly affect infrared spectra or X-ray powder diffraction patterns (vide infra), although it does increase the chain length somewhat (vide infra). Elemental analysis of typical polymer samples indicates that small traces of chloride are still present. Soxhlet extraction under inert atmosphere with dry CH_2Cl_2 or pyridine removes traces of soluble material which is found to be a mixture of $Si(Pc)(OH)_2$ and $HOSi(Pc)OSi(Pc)OH$[29] by UV–visible spectrophotometry. These impurities will be seen to have a negligible effect on collective properties.[14]

Preparation of the $[Ge(Pc)O]_n$ polymer is more straightforward. The $M(Pc)Cl_2$ compounds can be prepared from phthalonitrile in good yield and purity (Scheme I). The reaction mixtures must again be brought to reflux quickly, however, in order to minimize the decomposition of phthalonitrile and the solvent. As found for $Si(Pc)Cl_2$, hydrolysis in solution is rapid. Dehydration of the $M(Pc)(OH)_2$ compounds was monitored in a manner similar to the method described above for $Si(Pc)(OH)_2$. Polymerization of $Ge(Pc)(OH)_2$ for ca. 10 h at 440 °C gives complete reaction based on the disappearance of the Ge–O stretch (vide infra) at 642 cm^{-1} in the infrared spectrum of $Ge(Pc)(OH)_2$. Longer reaction times and/or higher temperatures do not affect the spectrum, although there is an increase in chain length (vide infra). The $Sn(Pc)(OH)_2$ monomer begins to undergo dehydration at 325 °C based upon the disappearance of the Sn–O stretch (vide infra) at 564 cm^{-1}

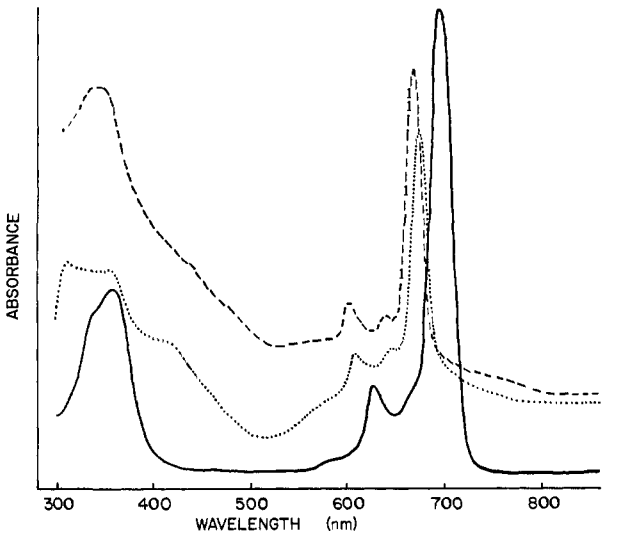

Figure 3. Electronic absorption spectra of $Si(Pc)(OH)_2$ (--), $Ge(Pc)(OH)_2$ (···), and $Sn(Pc)(OH)_2$ (—) in pyridine solution.

in the infrared spectrum of $Sn(Pc)(OH)_2$. The polymerization of $Sn(Pc)(OH)_2$ is apparently accompanied by some decomposition[30a] (vide infra) however, so the reaction is best carried out at the lowest temperature and for the shortest time beyond which there was no significant change in the infrared spectrum. Those conditions were found to be 30 min at 325 °C. Elemental analyses were consistently low in carbon for this material (see Experimental Section).

The polymer $[Si(Pc)O]_n$ was found to be soluble in concentrated H_2SO_4 and HSO_3CH_3. The polymer can be recovered from these acids without detectable change.[30b] Thus, under nitrogen, 0.013 g can be dissolved in 25 mL of concentrated H_2SO_4 after 90 min stirring at room temperature, and 0.020 g can be dissolved after 90 min stirring at 80 °C. Suction filtration of the resulting solution through an analytical fritted crucible into ice water yields a flocculent, blue-purple precipitate. Isolation by centrifugation, washing with water, and vacuum drying yields $[Si(Pc)O]_n$. Fourier transform infrared spectra of this material gives no evidence of ring sulfonation[31] or decrease in the number average degree of polymerization (vide infra). No changes are evident in X-ray diffraction (vide infra) or transport measurements.[14] Solubility in concentrated acid is of course a typical phthalocyanine property, and precipitation from H_2SO_4 is a common purification technique for M(Pc) derivatives of metals with high charge-to-radius ratios.[32] Siloxanes, on the other hand, are cleaved by sulfuric acid to yield silicon bisulfates.[33] Thus, it appears that the Si–O functionalities in $[Si(Pc)O]_n$ are significantly shielded by the bulk and close proximity of the cofacial phthalocyanine rings. Possibly as a consequence of the longer M–O distances among other factors, $[Ge(Pc)O]_n$ and $[Sn(Pc)O]_n$ were found to decompose in H_2SO_4.

Spectroscopic and Structural Properties of $M(Pc)Cl_2$, $M(Pc)(OH)_2$, and $[M(Pc)O]_n$ Compounds. Optical Spectra. It was of central interest in this investigation to determine the degree to which the structural model portrayed in Figure 1 is valid for the $[M(Pc)O]_n$ polymers. Important issues include verifying that

(28) Markova, I. Ya.; Popov, Yu. A.; Shaulov, Yu. Kh. *Russ. J. Phys. Chem.* (*Engl. Transl.*) **1970**, *44*, 1501–1502.

(29) Doris, K.; Marks, T. J.; Ratner, M. A., manuscript in preparation.

(30) (a) This has been noted previously. See ref 19c. (b) Dissolution in HSO_3CF_3 appears to result in partial oxidation of the polymer: Inabe, T.; Lyding, J. W.; Kannewurf, C. R.; Marks, T. J., manuscript in preparation.

(31) (a) There were no additional absorptions observed in the region 1030–1430 cm^{-1}, characteristic of an S=O stretching mode (see ref 31b). (b) Pouchert, C. J. "Aldrich Library of Infrared Spectra"; Aldrich Chemical Co.: Milwaukee, WI, 1970; p 839.

(32) Moser, F. H.; Thomas, A. L. "Phthalocyanine Compounds"; Reinhold: New York, 1963; pp 153–157.

(33) (a) Eaborn, C. "Organosilicon Compounds"; Butterworths: London, 1960; pp 259–262, 318–319. (b) Rochow, E. G. In "Comprehensive Inorganic Chemistry"; Bailar, H. C., Emeleus, H. J., Nyholm, R., Trotman-Dickenson, A. F., Eds.; Pergamon Press: Oxford, 1973; Vol. 3, pp 1458–1460. (c) Voronkov, Yu. A.; Mileshkevich, V. P. "The Siloxane Bond"; Consultants Bureau: New York, 1978; Chapter 2.

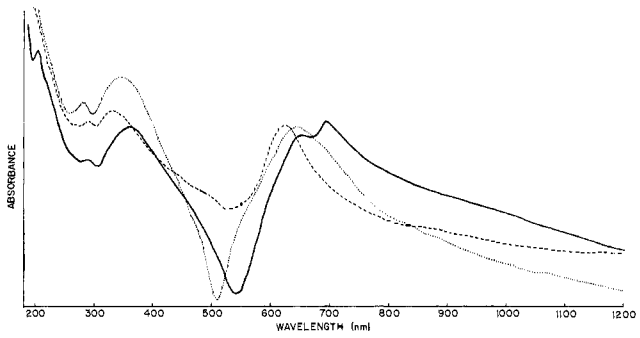

Figure 4. Electronic absorption spectra of $[Si(Pc)O]_n$ (--), $[Ge(Pc)O]_n$ (···), and $[Sn(Pc)O]_n$ (—) as Nujol mulls.

Table I. Optical Absorption Spectral Data for $M(Pc)(OH)_2$ and $[M(Pc)O]_n$ Compounds

compd	absorption maxima, nm
$Si(Pc)(OH)_2$[a]	340, 445, 602 w, 640 w, 671
$[Si(Pc)O]_n$[b]	203, 285, 335, 625
$Ge(Pc)(OH)_2$[a]	315, 358, 415, 607 w, 645 w, 676
$[Ge(Pc)O]_n$[b]	285, 350, 645
$Sn(Pc)(OH)_2$[a]	340, 360, 626 w, 665 w, 696
$[Sn(Pc)O]_n$[b]	205, 290, 365, 655, 695

[a] Pyridine solutions; w = weak transition. [b] Nujol mulls.

the molecular connectivity is as portrayed, obtaining data on the degree of polymerization, obtaining metrical information on electronic structure and macromolecular architecture as M is varied, and acquiring reference data for the subsequent studies of the partially oxidized materials.

Solution optical spectra of $Si(Pc)(OH)_2$, $Ge(Pc)(OH)_2$, and $Sn(Pc)(OH)_2$ are shown in Figure 3 and are typical of M(Pc) complexes. Phthalocyanine optical spectra[34,35] can be understood in terms of a porphyrinic "four orbital" model,[34,36] with $\pi \rightarrow \pi^*$ α (or Q) band transitions at ca. 670 nm (the shoulders at 625 and 675 nm are likely of vibronic origin) and Soret-like (or B) $\pi \rightarrow \pi^*$ bands near 340 nm. It can be seen that the transition Si → Ge → Sn results in a progressive red shift of the lowest energy $\pi \rightarrow \pi^*$ excitation. Such trends are explicable in terms of decreasing electronegativity of M, which shifts charge onto the ring and raises the energy of the $a_{2u}(\pi)$ HOMO.[37] An analogous effect is observed upon alkyl substitution of the phthalocyanine skeleton.[38] As can be seen from the $[M(Pc)O]_n$ spectra in Figure 4, the same M trends in the α band energies persist in the solid state. Judging from optical spectroscopic results on face-to-face ROSi(Pc)-OSi(Pc)OR dimers,[29,39] excitonic shifts in the α band are not expected to be large and such is the case. That the $[M(Pc)O]_n$ systems do not exhibit great splitting of this band as is observed for Ni(Pc) is in excellent accord with the explanation[40] that the splitting in the latter system arises from the low (non-D_{4h}, slipped stack) site symmetry. The slight splitting in the $[Sn(Pc)O]_n$ spectrum may arise from the large size of the Sn(IV) ion and

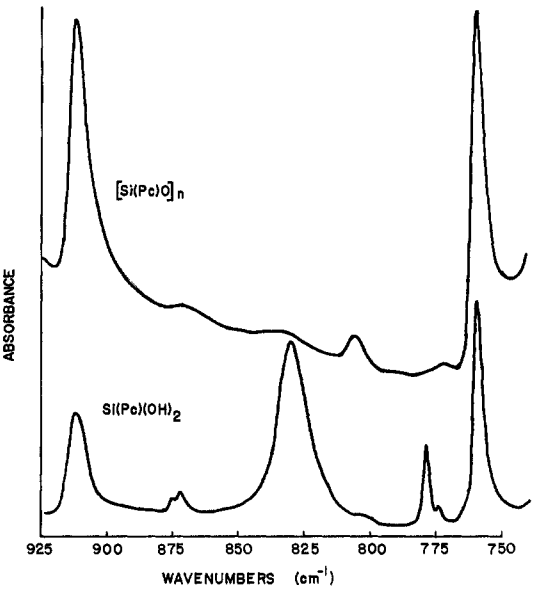

Figure 5. Fourier transform infrared spectra of $Si(Pc)(OH)_2$ and $[Si(Pc)O]_n$.

consequent buckling of the ring[41] as found in the crystal structure of $Sn(Pc)Cl_2$;[22b] however, this distortion is not evident in the $Sn(Pc)Cl_2$ and $Sn(Pc)(OH)_2$ solution spectra.[42] Optical spectral data are compiled in Table I.

Spectroscopic and Structural Properties of $M(Pc)Cl_2$, $M(Pc)(OH)_2$, and $[M(Pc)O]_n$ Compounds. Vibrational Spectra and Quantitative End Group Analysis. There is an extensive literature[43-45] on phthalocyanine vibrational spectra, and the $M(Pc)Cl_2$, $M(Pc)(OH)_2$, and $[M(Pc)O]_n$ compounds conform well to published criteria, differing only, for constant M, in transitions attributable to the axial ligands. Assignments are set out in Table II, using the numbering scheme of Sidorov and Kotlyar.[43] Thus, the transitions generally regarded as being sensitive to metal ion are those numbered 13, 17, 27, 30, and 31. Peak numbers 5, 8, 9, 11, 12, 14, 19, 22, and 23 are characteristic of a metalated phthalocyanine but are not sensitive to the particular metal ion present. In terms of internal coordinate changes, the following assignments can be made.[43-45] C–H out-of-plane bending 5, 10, 11, 12; C–H in-plane bending 17, 20, 21; C–N stretch 18; C–C stretch 31, 32; C–C ring deformation 1,2, 3, 4.

To assess the number average molecular weight ($\bar{M}_n$), a quantitative spectrophotometric end group analysis was conducted in which the intensity of the M–O stretching mode in the $M(Pc)(OH)_2$ compounds was compared to residual absorption by the polymer in that spectral region. This approach makes the physically reasonable assumption that, relative to essentially invariant Pc skeletal modes, the M–O(hydroxy) stretching frequency and transition dipole for the monomer should be approximately the same as the terminus of an $[M(Pc)O]_nM(Pc)OH$ fragment. It was also of interest to identify polymer backbone frequencies for future investigations of electron–phonon coupling. The spectral region of interest in $Si(Pc)(OH)_2$ and $[Si(Pc)O]_n$ is shown in Figure 5. The vibrations at 911, 875, 872, 804, 780, 775, and 758 cm^{-1} in $Si(Pc)(OH)_2$ can be assigned (vide infra) to phthalocyanine transition numbers 13, 12, 11, 10, 9, 8, and 6. The same absorptions are observed in $Si(Pc)Cl_2$. The remaining, intense absorption at 830 cm^{-1} in the $Si(Pc)(^{16}OH)_2$ spectrum is

(34) Gouterman, M. *Porphyrins* **1978**, *3*, 1–163.
(35) (a) Schaffer, A. M.; Gouterman, M.: Davidson, E. R. *Theor. Chim. Acta* **1973**, *30*, 9–30. (b) Schaffer, A. M.; Gouterman, M. *Ibid.* **1972**, *25*, 62–70. (c) Edwards, L.; Gouterman, M. *J. Mol. Spectrosc.* **1970**, *33*, 292–310. (d) Chem, I. *Ibid.* **1967**, *23*, 131–143.
(36) (a) Case, D. A.; Karplus, M. *J. Am. Chem. Soc.* **1977**, *99*, 6182–6184. (b) Stillman, M. J.; Thompson, A. J. *J. Chem. Soc., Faraday Trans. 2* **1974**, *70*, 790–804, 805–814. (c) Chantrell, S. J.; McAuliffe, C. A.; Munn, R. W.; Pratt, A. C. *Coord. Chem. Rev.* **1975**, *16*, 259–284 and references cited therein. (d) Eaton, W. A.; Hochstrasser, R. M. *J. Chem. Phys.* **1968**, *49*, 985–995. (e) Gouterman, M. *J. Mol. Spectrosc.* **1961**, *6*, 138–163.
(37) (a) Gouterman, M. *J. Chem. Phys.* **1959**, *30*, 1139–1161. (b) Gouterman, M.; Schwarz, F. P.; Smith, P. D.; Dolphin, D. *J. Chem. Phys.* **1973**, *59*, 676–690.
(38) Cuellar, E. A.; Marks, T. J. *Inorg. Chem.* **1981**, *20*, 3766–3770.
(39) Hush, N. S.; Woolsey, J. S. *Mol. Phys.* **1971**, *21*, 465–474. Here the shift is estimated to be +37 nm.
(40) Day, P.; Scregg, G.; Williams, R. J. P. *J. Chem. Phys.* **1963**, *38*, 2778–2779.
(41) Marks, T. J.; Stojakovic, D. R. *J. Am. Chem. Soc.* **1978**, *100*, 1695–1705 and references therein.
(42) (a) Large distortions as in $Pb(Pc)$[42b] are usually detectable in the optical spectra.[35c] (b) Ukei, K. *Acta Crystallogr., Sect. B* **1973**, *B29*, 2290–2292.
(43) Sidorov, A. N.; Kotlyar, I. P. *Opt. Spektrosk.* **1961**, *11*, 175–184.
(44) Kobayashi, T.; Kurokawa, F.; Uyeda, N.; Suito, E. *Spectrochim. Acta, Part A* **1970**, *26A*, 1305–1311.
(45) Steinbach, F.; Joswig, H.-J. *J. Chem. Soc., Faraday Trans. I* **1979**, *75*, 2594–2600.

Table II. Infrared Spectral Data for $M(Pc)Cl_2$, $M(Pc)(OH)_2$, and $[M(Pc)O]_n$ Compounds

	$Si(Pc)Cl_2$	$Si(Pc)(OH)_2$	$[Si(Pc)O]_n$	$Ge(Pc)Cl_2$	$Ge(Pc)(OH)_2$	$[Ge(Pc)O]_n$	$Sn(Pc)Cl_2$	$Sn(Pc)(OH)_2$	$[Sn(Pc)O]_n$
	383[a] s						345[a] w		
	418 m			425 w	425 vw	425 vw			428 w
	430 s								
1	438 sh	450 w		437 w		435 vw	435 w	438 m	435 sh
	468[a] vs						447[a] m		
2	509 w			512 m	506 m	508 m	500 m	500 m	495 m
	533[a] s	530[a] m	530[a] m					562[a] s	
3	574 m	575 m	575 m	574 m	568 m	572 m	574 s	573 sh	570 m
	609[a] w	617[a] w		610[a] w	615[a] w				
4	647 m	644 m	646 w	641 w	640 w	640 w	640 w	640 w	640 w
					646[a] s				
		674 w			672 w	660 vw	670 w	675 w	660 vw
	692 m	701 w		688 m	695 vw			699 m	687 vw
5	730 vs	728 vs	721 vs	723 vs	727 vs	725 vs	720 vs	718 vs	716 vs
6	760 s	758 vs	759 vs	754 s	757 vs	753 m	748 s	750 s	750 s
			762[a] w			762[a] vw			762[a] m
8	774 w	775 w		768 w	769 m	772 vw	771 m	768 m	769 m
9	783 s	780 s		780 s	778 m		778 s	777 m	775 sh
10	808 w	804 sh	804 w	803 w	800 w	801 w	805 w	805 w	808 m
		830[a] vs				865[a] bd			825[a] bd
11	867 m	872 w	869 vw	868 m	870 w				872 w
12	882 m	875 w		884 m					
13	912 s	911 m	910 s	902 s	903 s	899 s	888 s	890 s	888 m
14			936[a] vw			935[a] vw			
15		951 w			950 m	945 vw			950 w
	960 m			960 w			959 w	957 w	
	987[a] w	976[a] w		988[a] vw	988[a] w	970[a] vw		980[a] w	
	1004 w	991 w	1000[a] bd	1005 vw	1005 w	998 w	990 w	1005 w	1005 vw
		1020[a] w			1022[a] vw				
	1050 sh		1043 m	1054 sh					
17	1060 s	1072 vs				1068 vs	1058 s	1051 s	1058 s
18	1080 vs	1077 vs	1080 vs	1078 vs	1073 vs	1087 vs	1083 vs	1082 vs	1089 s
19				1098 w	1097 w				
20	1120 vs	1119 s	1121 vs	1120 vs	1119 s	1119 vs	1120 s	1115 s	1120 vs
		1134 m			1132 s			1130 m	
21	1162 s	1166 m	1164 s	1162 m	1167 m	1162 s		1165 m	1168 m
			1170 sh		1178 w		1171 m	1177 sh	
			1192 w		1200 w	1195 w		1190 w	1183 w
	1240[a] vw	1223[a] w							1263[a] w
23	1290 s	1290 s	1289 s	1287 s	1290 s	1284 m	1288 s	1282 s	1284 m
								1293[a] w	1293[a] w
26	1336 vs	1335 vs	1334 vs	1333 vs	1335 vs	1332 vs		1330 s	1338 vs
	1342[a] sh			1340[a] sh	1347[a] m	1345[a] m	1347[a] vs	1340[a] sh	
	1352[a] sh		1351[a] m	1353[a] w				1345[a] s	
27	1430 s	1431 s	1426 vs	1423 s	1422 m	1419 s	1408 m	1404 m	1405 sh
30	1532 s	1518 s	1517 s	1510 s	1499 s	1500 m			
31	1595 sh	1595 w	1596 w	1590 w	1585 w	1588 w	1590 sh		1580 sh
32	1610 m	1609 m	1614 m	1610 m	1605 m	1612 m	1608 w	1609 m	1610 m

[a] Peaks not readily assigned to M(Pc) moiety (based on ref 43 and 44). Numbered according to ref 43. s = strong, m = medium, w = weak, bd = broad, sh = shoulder, v = very.

assigned to the locally ^{16}O–Si–^{16}O antisymmetric stretch. Such transitions generally occur in the 830–950-cm^{-1} region for monomeric silanols.[46] In $Si(Pc)(^{18}OH)_2$, this vibration shifts to 808 cm^{-1}, confirming the assignment.[47] As can be seen in Figure 5, the 830-cm^{-1} band disappears upon polymerization. The only new Si–O-related transition to appear is a broad band centered at 1000 cm^{-1}; this is assigned to the (locally[48]) antisymmetric Si–O–Si stretch.[46,49] Such transitions typically occur at 1000–1130 cm^{-1} in siloxanes, and frequently broaden or split with increasing molecular weight.[46] In $[Si(Pc)^{18}O]_n$, this transition shifts[47] to 950

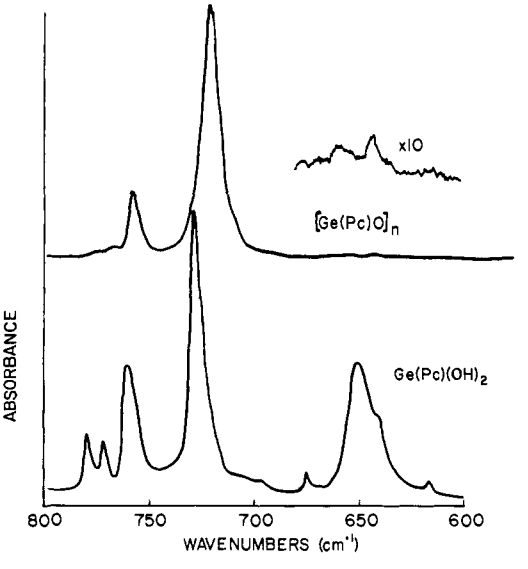

Figure 6. Infrared spectra of $Ge(Pc)(OH)_2$ and $[Ge(Pc)O]_n$.

(46) (a) Smith, A. L. "Analysis of Silicones"; Wiley: New York, 1974; pp 275–279. (b) See also: Joyner, R.; Kenney, M. E. *Inorg. Chem.* **1962**, *1*, 717–718.

(47) A simple diatomic, harmonic oscillator calculation predicts a shift of ν_{Si-O} to 800 cm^{-1} for $Si(Pc)(^{18}OH)_2$ and to 964 cm^{-1} for $[Si(Pc)^{18}O]_n$.

(48) Formally, this transition should be described in terms of the optical branch of the dispersion relation for the polymer chain. (a) Turrell, G. "Infrared and Raman Spectra of Crystals"; Academic Press: New York, 1972; Chapters 3,7. (b) Koenig, J. L. "Chemical Microstructure of Polymer Chains"; Wiley-Interscience: New York, 1980; Chapter 7.

(49) (a) Maslowsky, E., Jr. "Vibrational Spectra of Organometallic Compounds"; Wiley: New York, 1977; pp 107–118. (b) Esposito, J. N.; Sutton, L. E.; Kenney, M. E. *Inorg. Chem.* **1967**, *6*, 1116–1120.

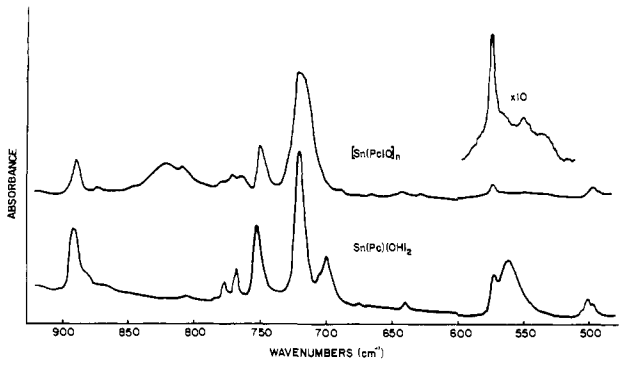

Figure 7. Infrared spectra of $Sn(Pc)(OH)_2$ and $[Sn(Pc)O]_n$.

cm^{-1} (also broad), confirming the assignment.

Portions of the $Ge(Pc)(OH)_2$ and $[Ge(Pc)O]_n$ infrared spectra are shown in Figure 6. The transitions at 778, 769, 757, 727, and 640 cm^{-1} in $Ge(Pc)(OH)_2$ are assigned to phthalocyanine peak numbers 9, 8, 6, 5, and 4, respectively, and are also observed in $Ge(Pc)Cl_2$. The weak absorptions at 695 and 672 cm^{-1} are also commonly observed phthalocyanine absorptions and are found in each $M(Pc)(OH)_2$ spectrum. The Ge–O asymmetric stretch is assigned at 646 cm^{-1}, which is a typical value for germanols.[49] Upon polymerization, the only strong absorptions remaining in this region are the phthalocyanine absorptions at 753 and 725 cm^{-1}. The weak phthalocyanine transitions at 640 and 660 cm^{-1} are approximately the same intensity as the Ge–O remnant at 646 cm^{-1} in the $[Ge(Pc)O]_n$. This factor complicates somewhat the molecular weight estimation as compared to $Si(Pc)(OH)_2$ in which the Si–O stretch occurs in a spectral region free of other absorptions (vide infra). The locally antisymmetric Ge–O–Ge stretch in $[Ge(Pc)O]_n$ is assigned to the broad peak at 865 cm^{-1}, a reasonable assignment for germoxanes.[49]

The infrared spectra of $Sn(Pc)(OH)_2$ and $[Sn(Pc)O]_n$ are shown in Figure 7. The peaks at 890, 805, 777, 768, 750, 718, 640, 573, and 500 cm^{-1} in $Sn(Pc)(OH)_2$ are assigned to phthalocyanine transitions number 13, 10 9, 8, 6, 5, 4, 3, and 2, respectively. These absorptions are also observed in $Sn(Pc)Cl_2$; weak phthalocyanine absorptions at 699 and 675 cm^{-1} are also present. Information on vibrational spectra of stannols is not generally available as most are polymers with bridging oxygens. The Sn–O stretch has been assigned at positions from 575 to 912 cm^{-1} in stannols and stannoxanes.[49,50] We assign the antisymmetric Sn–O stretch in $Sn(Pc)(OH)_2$ at 562 cm^{-1}. This peak disappears on polymerization and a broad absorption grows in at 825 cm^{-1}, which can be assigned to the antisymmetric O–Sn–O stretch in $[Sn(Pc)O]_n$. Other bands in the spectrum are assigned to phthalocyanine modes described above. As is the case with $[Ge(Pc)O]_n$, the remnant of the Sn–O stretch at 560 cm^{-1} is near a phthalocyanine absorption at 570 cm^{-1} in the $[Sn(Pc)O]_n$ spectrum.

For the end group analysis, calculation of maximum residual OH concentration in the $[M(Pc)O]_n$ materials was performed by quantitatively determining the relative $\nu_{M-O(hydroxy)}$ areas in the monomer and polymer infrared spectra relative to essentially invariant Pc skeletal modes in the same region of the spectrum. The number average degree of polymerization was then calculated, assuming the reaction shown in eq 2. In the case of $Si(Pc)(OH)_2$,

$$n\mathrm{M(Pc)(OH)_2} \xrightarrow[\Delta]{} \mathrm{HO[M(Pc)\text{–}O]_n\text{–}H} + (n-1)\mathrm{H_2O} \quad (2)$$

the Si–O stretch at 830 cm^{-1} was measured with respect to phthalocyanine modes at 758 and 911 cm^{-1} (numbers 6 and 13). The results for these two "standards" agreed to within 10%, and yield, for several $[Si(Pc)O]_n$ samples, a value of $n = 120$ (30). The end group analysis for $[Ge(Pc)O]_n$ was complicated by the presence of phthalocyanine absorptions near the Ge–O stretch, as mentioned earlier. The Ge–O stretch at 646 cm^{-1} was measured

(50) (a) Poller, R. C. *J. Inorg. Nucl. Chem.* **1962**, *24*, 593–600. (b) See: Kroenke, W. J.; Kenney, M. E. *Inorg. Chem.* **1964**, *3*, 696–698 for a similar conclusion.

Table III. Number Average Molecular Weight Data for $[M(Pc)O]_n$ Polymers

polymer	polymerization conditions[a] temp, °C	time, h	n by IR end group analysis	n by tritium labeling
$[Si(Pc)O]_n$	440	1	120 (30)	66.5
	440	12	120 (30)	102
	420	48		133
	420	120		139
$[Ge(Pc)O]_n$	400	11		8.0
	410	3		11.3
	430	3		11.4
	440	10	70 (40)	62.0
	440	48		86.4
$[Sn(Pc)O]_n$	325	0.5	100 (40)	14.6

[a] At 10^{-3} torr.

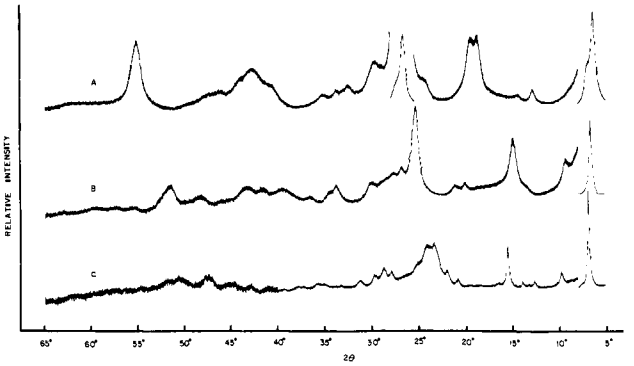

Figure 8. X-ray diffraction data for polycrystalline samples of (A) $[Si(Pc)O]_n$, (B) $[Ge(Pc)O]_n$, (C) $[Sn(Pc)O]_n$. Vertical scale settings in thousands of counts per second: (A) 5–8°, 10 kcps; 8–25.5°, 2 kcps; 25.5–28°, 20 kcps; 28–65°, 2 kcps; (B) 5–8°, 20 kcps; 8–22°, 2 kcps; 22–29°, 4 kcps; 29–65°, 2 kcps; (C) 5–8°, 4 kcps; 8–40°, 2 kcps; 40–65°, 1 kcps.

with respect to the phthalocyanine transitions at 757 and 727 cm^{-1}, and the result is $n = 70$ (40). The Sn–O stretch in $Sn(Pc)(OH)_2$ is also in the proximity of phthalocyanine absorptions. The Sn–O stretch at 562 cm^{-1} was measured with respect to the phthalocyanine modes at 892 and 752 cm^{-1}, and analysis of these data yields $n = 100$ (40). Preliminary solution laser light scattering measurements on $[Si(Pc)O]_n$ yield $n \approx 100$ in H_2SO_4.[51] Molecular weight data are compiled in Table III.

Molecular Weights by Tritium Labeling. Additional information on $[M(Pc)O]_n$ $\bar{M}_n$ values as well as a calibration of the easily acquired spectrophotometric end group analysis data was obtained via tritium labeling[52] studies. Labeled monomer was prepared as shown in eq 3, and the tritium content compared to that in the

$$\mathrm{M(Pc)Cl_2} + 2\mathrm{O^3H^-} \rightarrow \mathrm{M(Pc)(O^3H)_2} + 2\mathrm{Cl^-} \quad (3)$$

polymer, assuming the process shown in eq 4. Results are

$$n\mathrm{M(Pc)(O^3H)_2} \rightarrow {}^3\mathrm{HO[M(Pc)O]}_n{}^3\mathrm{H} + (n-1){}^3\mathrm{H_2O} \quad (4)$$

presented in Table III. The agreement between duplicate measurements was excellent (within 5%) and the agreement between tritium labeling and infrared end group analysis $\bar{M}_n$ values is generally favorable except in the case of $[Sn(Pc)O]_n$ (where decomposition may be occurring). The tritium labeling experiments indicate that longer polymerization times and high temperatures generally increase the molecular weights, thus offering an obvious means for controlling $\bar{M}_n$.

$[M(Pc)O]_n$ Crystal Structure Analysis. The rich, sharp X-ray powder diffraction patterns of the $[M(Pc)O]_n$ materials (Figure

(51) Berry, G. C., private communication.

(52) For a general discussion of such techniques, see: (a) Clark, H. M. In "Techniques of Chemistry"; Weissberger, A., Ed.; Wiley: New York, 1972; Vol. I, Part IIID, pp 587–659. (b) Ayrey, G. *Adv. Polym. Sci.* **1969**, *6*, 128–148. (c) Feinendegen, L. E. "Tritium-Labelled Molecules in Biology and Medicine"; Academic Press: New York, 1967.

8) are indicative of appreciable crystallinity (in contrast to most conductive polymer systems[13,53]) and suggest, in the absence of suitable polymer single crystals or highly oriented fibers, that structural information might be obtainable which would allow further testing of the validity of the structural model shown in Figure 1. Analysis of the diffraction data (see Experimental Section for further details) employed judiciously chosen model compounds as well as several computer programs, one of which generates theoretical powder patterns for hypothetical crystal structures. The model compounds included a number of mononuclear metallophthalocyanines[2,23b] and metalloporphyrins.[24] Also of particular relevance is the isoelectronic, cofacial polymer $[Ga(Pc)F]_n$ ($P\bar{1}$, a = 3.8711 (3) Å, b = 12.601 (1) Å, c = 12.793 (1) Å, α = 90.271 (1)°, β = 96.42 (1)°, γ = 91.28 (1)°) which crystallizes with stacks of nearly *eclipsed* Ga(Pc) units arrayed at 3.87-Å interplanar distances and connected by symmetrical, linear Ga–F–Ga bridges (F).[23a,54] Also of interest is the crystal

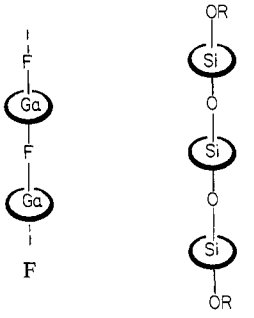

F G

structure of $[(CH_3)_3SiO]_2(CH_3)SiO[Si(Pc)O]_3Si(CH_3)[OSi(CH_3)_3]_2$,[23c] which can be thought of as a three-ring subunit of $[Si(Pc)O]_n$ (G). The Si–O–Si backbone is linear, with neighboring Pc rings staggered by 16° and an interplanar spacing (Si–Si distance) of 3.324 (4) Å. The two outer Pc rings are each buckled slightly away from the central ring. The final model compound is valid for discussion of both undoped as well as doped[14a] polymer crystal structures. $Ni(Pc)I_{1.0}$ crystallizes in the tetragonal space group $P4/mcc$, with Z = 2, and the unit cell constants a = 13.936 (6) Å, c = 6.488 (3) Å. In this case, the phthalocyanine rings are stacked at 3.244 (2) Å intervals and are staggered by 39.6° with respect to adjacent rings in the same stack. There are channels containing chains of I_3^- ions which extend parallel to the $Ni(Pc)^{0.33+}$ stack.

The analysis of the $[M(Pc)O]_n$ diffraction data makes the physically reasonable assumption that the polymer architecture can be described by a single structure in which the M(Pc) internal dimensions are the same as those in metallophthalocyanines with M ions of the same or comparable ionic radius, and that the M–O–M vectors are linear (for which there is considerable precedent[23c,25]) and perpendicular to the M(Pc) ring planes[55] (for which there is considerable precedent). Parameters which were varied included the interplanar spacing, the eclipsing angle between neighboring rings in a stack (ϕ, H), the angle between the Pc trans

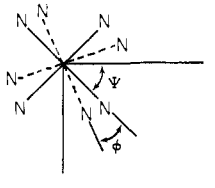

H

(53) (a) Shacklett, L. W.; Eckhardt, H.; Chance, R. R.; Miller, G. G.; Ivory, D. M.; Baughman, R. H. In ref 13e; pp 115–123. (b) Baughman, R. H.; Hsu, S. L.; Anderson, L. R.; Pez, G. P. In ref 1d; pp 187–201. (c) Chance, R. R.; Shacklette, L. W.; Eckhardt, H.; Sowa, J. M.; Elsenbaumer, R. L.; Ivory, D. M.; Miller, G. G.; Baughman, R. H. In ref 13e; pp 125–135.

(54) The Ga–F–Ga vector makes an angle of 96° with respect to the Ga(Pc) plane, so that the stacking is slightly slipped.[23a]

(55) This is true for $Si(Pc)[OSi(CH_3)_3]_2$,[23b] trimer C,[23c] and Ge(porphyrinato)$(OCH_3)_2$.[24a]

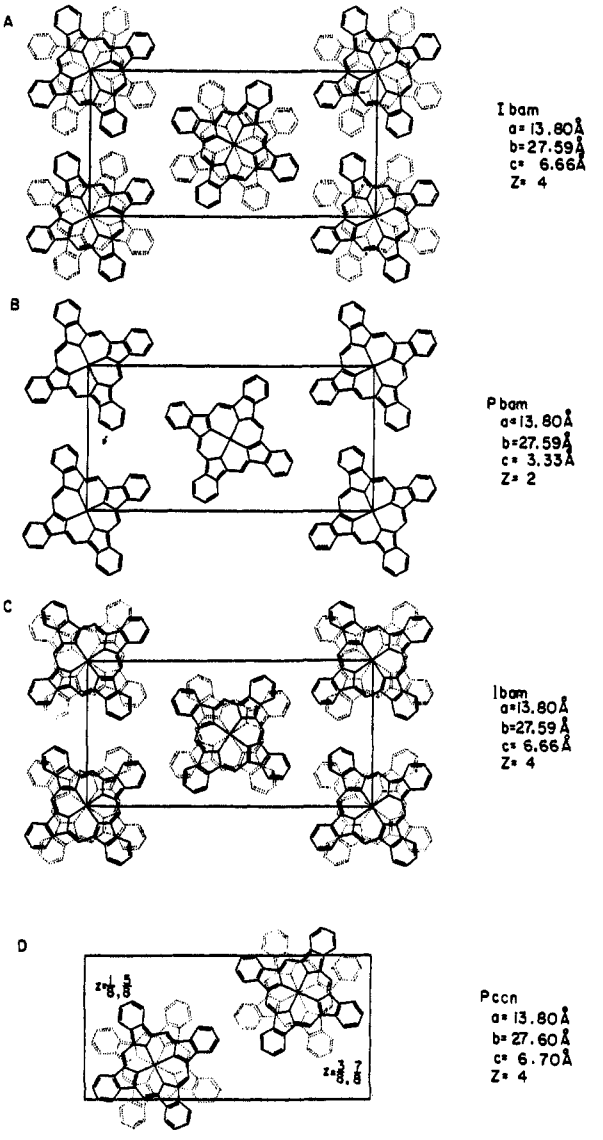

Figure 9. Diagrams of several $[Si(Pc)O]_n$ crystal structures considered in the analysis of the X-ray diffraction data.

N–M–N vector and the unit cell edge (ψ, H), and the relative orientations of the linear polymer chains within the unit cell.

Beginning with the $[Si(Pc)O]_n$ diffraction data, it was quickly determined that the powder pattern could not be fit with simple (primitive) tetragonal (eclipsed (Z = 1) or staggered (Z = 2) Si(Pc) rings) or orthorhombic (eclipsed (Z = 1) or staggered (Z = 2) Si(Pc) rings) crystal structures, nor to cells of appreciably lower symmetry. Moreover, the lattice parameters which were derived in the orthorhombic fitting attempts resulted in unrealistic interstack nonbonding H–H contacts (≤1.6 Å vs. the normal van der Waals distance of 2.4–2.9 Å[56]). A number of larger orthorhombic cells were next investigated, carefully varying ϕ and ψ. Molecular models were employed to assess interstack nonbonded contacts in each new configuration. Representative structural arrangements and the corresponding fits are set out in Figures 9 and 10, respecively. The simplest crystal structure which conforms to the constraints imposed by the model compounds and which agree with the experimental data is shown in Figure 9A (fit in Figure 10A). Cell parameters and the measured density (in good agreement with the calculated density) are set out in Table IV. The derived interplanar spacing, 3.33 (2) Å, is in excellent agreement with that in the model trimer (C, 3.324 (4) Å) and from an earlier, far more qualitative analysis.[57a] The

(56) (a) Bondi, A. *J. Phys. Chem.* **1964**, *68*, 441–451. (b) Allinger, N. L. *J. Am. Chem. Soc.* **1968**, *90*, 1199–1210.

Table IV. Crystallographic Data for $[M(Pc)O]_n$ Materials

polymer	space group	Z	cell parameters, Å	density, g cm^{-3} calcd	density, g cm^{-3} found	interplanar spacing, Å	staggering angle (ϕ), deg
$[Si(Pc)O]_n$	*Ibam*	4	$a = 13.80$ (5), $b = 27.59$ (5), $c = 6.66$ (4)	1.458 (21)	1.432 (10)	3.33 (2)	39 (3)
$[Ge(Pc)O]_n$	*P4/m*	1	$a = 13.27$ (5), $c = 3.53$ (2)	1.609 (28)	1.512 (2)	3.53 (2)	0 (5)[a]
	I4/m	2	$a = 18.76$ (5), $c = 3.57$ (2)	1.589 (26)		3.57 (2)	0 (5)[a]
$[Sn(Pc)O]_n$[b]	*P4/m*	1	$a = 12.81$ (5), $c = 3.82$ (2)	1.715 (25)	1.719 (10)	3.82 (2)	probably eclipsed

[a] Formally this space group requires a staggering angle of 0°. [b] Parameters for trial structure in Figure 13B. See text for discussion of the optimum fit.

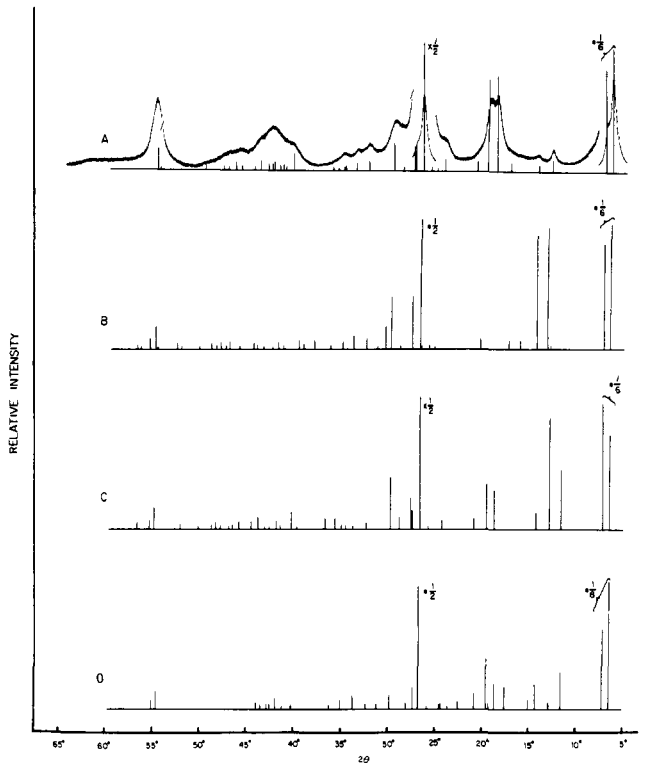

Figure 10. Computed X-ray powder diffraction patterns for the $[Si(Pc)O]_n$ structures shown in Figure 9. Letters correspond to the letters in Figure 9, and the experimental diffraction pattern is also shown in A.

staggering angle, $\phi = 39 \pm 3°$ ($\psi = 25 \pm 2°$) is somewhat larger than that in the trimer but comparable to that in $[Ni(Pc)]I_{1.0}$ (39.6°).[4b] It is likely that ring buckling or staggering represent alternative means to relieve intrastack ring–ring nonbonded repulsions in these systems, and with the polymeric $[Si(Pc)O]_n$ arrangement presumably rendering buckling less favorable than in C, increased staggering becomes favored. Attempts to fit the $[Si(Pc)O]_n$ diffraction data to structures with eclipsed rings (e.g., Figures 9B and 10B) or considerably reduced staggering angles (e.g., Figures 9C and 10C) were considerably less successful. "Interleaved" packing arrangements (e.g., Figures 9D and 10D) also produced less satisfactory fits. This polymer diffraction analysis is clearly not a substitute for a single-crystal diffraction study; however, it is important to note that, within the bounds of the starting assumptions, the $[Si(Pc)O]_n$ diffraction data can be explained by a reasonable structural model which is in accord with that portrayed in Figure 1, i.e., parallel chains of cofacially arrayed metallomacrocycles.

The analysis of the $[Ge(Pc)O]_n$ data proceeded along the lines described for the silicon polymer. It was found that the data could be readily fit to a simple tetragonal structure (Figures 11B and

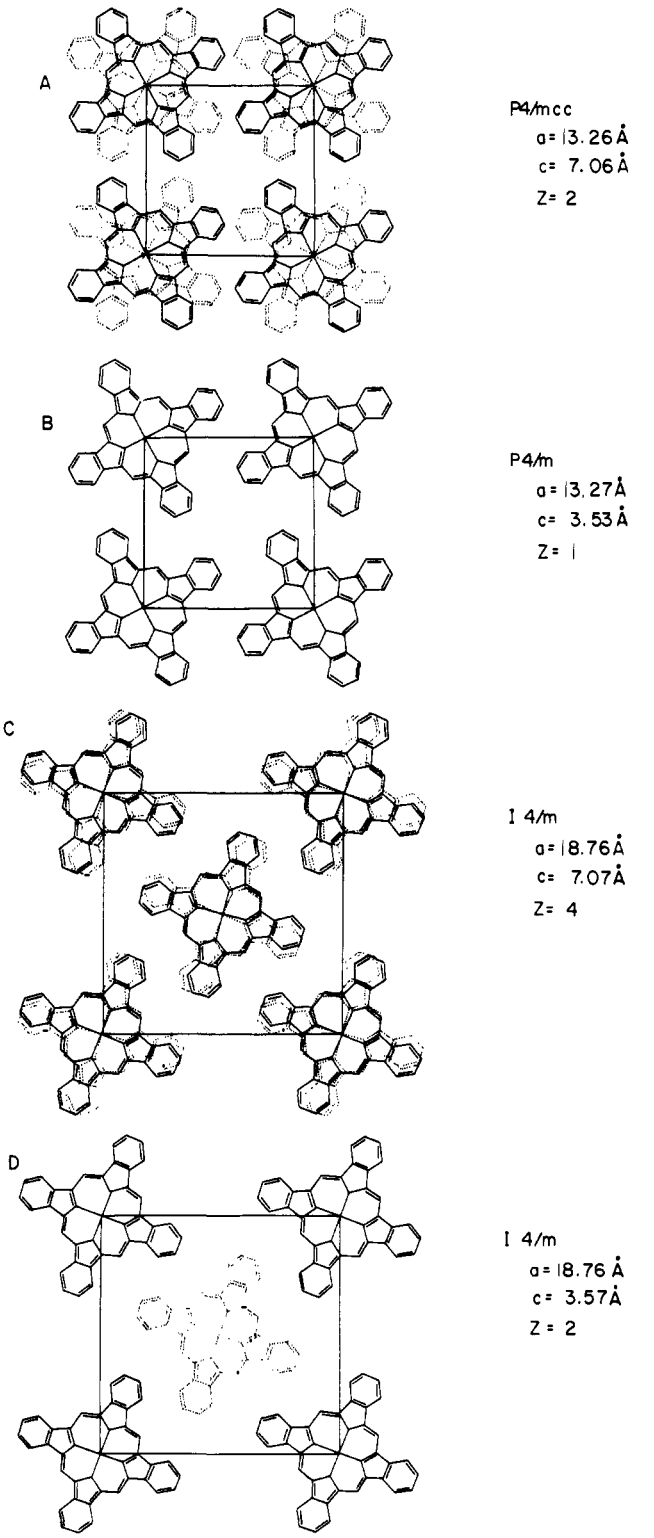

Figure 11. Diagrams of several $[Ge(Pc)O]_n$ crystal structures considered in the analysis of the X-ray diffraction data.

(57) (a) Kronenke, W. J.; Sutton, L. E.; Joyner, R. D.; Kenney, M. E. *Inorg. Chem.* **1963**, *5*, 1064–1065. (b) Nonbonded H–H interactions are somewhat less severe (~2 Å) in the body-centered structure of Figures 13A and 1A; however, the agreement between the theoretical and observed diffraction patterns in the $2\theta \approx 24°$ region is less satisfactory.

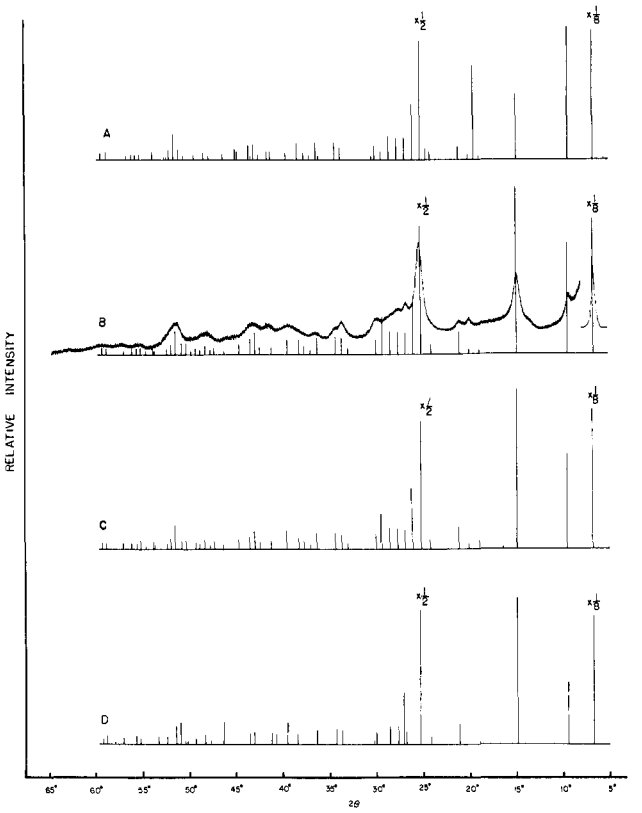

Figure 12. Computed X-ray powder diffraction patterns for the [Ge(Pc)O]$_n$ structures shown in Figure 11. Letters correspond to the letters in Figure 11, and the experimental diffraction pattern is shown in B.

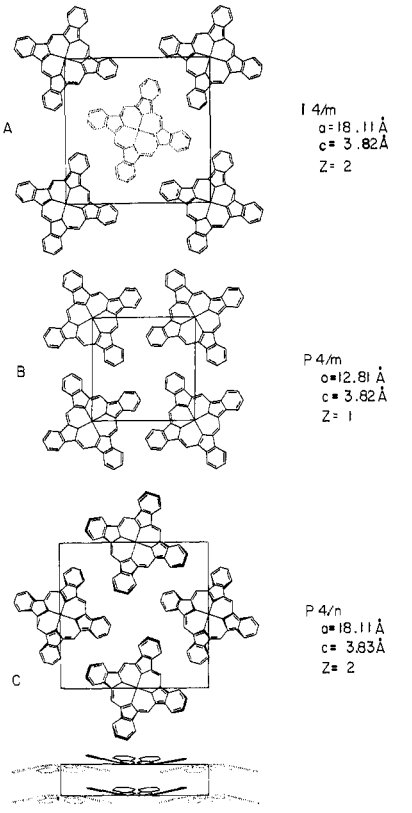

Figure 13. Diagrams of several [Sn(Pc)O]$_n$ crystal structures considered in the analysis of the X-ray diffraction data.

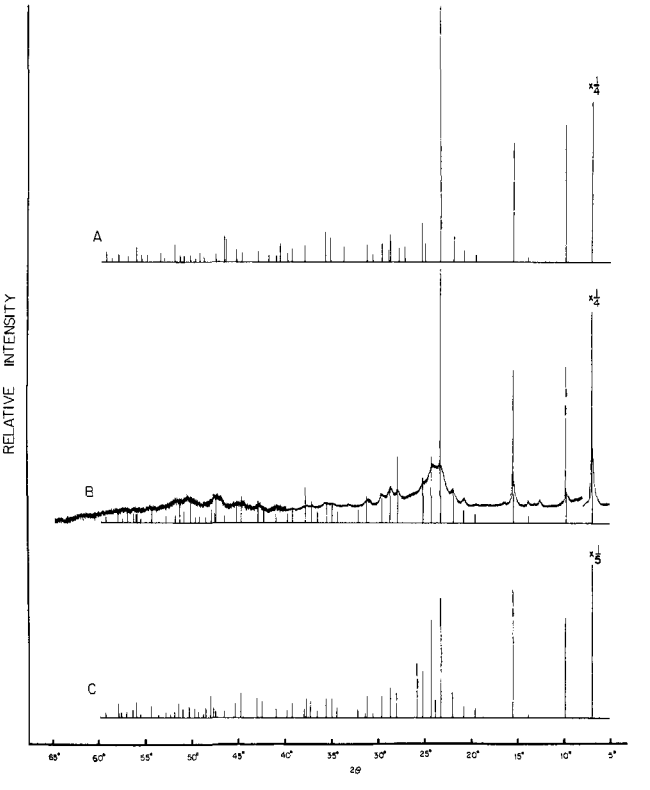

Figure 14. Computed X-ray powder diffraction patterns for the [Sn(Pc)O]$_n$ structures shown in Figure 13. Letters correspond to the letters in Figure 13, and the experimental diffraction pattern is also shown in B.

12B) with *eclipsed* rings. The derived interplanar spacing, 3.53 (2) Å, is in reasonable agreement with that calculated from the [Si(Pc)O]$_n$ structure, 3.59 Å, corrected for differences in ionic radii.[26] Attempts to fit the diffraction data to structures with staggering angles as large as in [Si(Pc)O]$_n$ were unsuccessful (e.g., Figures 11A and 12A), while intermediate angles led to severe nonbonded interstack H–H interactions. With nonprimitive cells, satisfactory fits could be obtained for small staggering angles (e.g., Figures 11C and 12C); however, calculated H–H contacts were rather short (1.77 Å, $\phi = 3°$; 1.73 Å, $\phi = 7°$; 1.77 Å, $\phi = 14°$). Even in an eclipsed structure of this type, several H–H contacts could not be brought above 1.87 Å, for any ψ value. Structures with Ge(Pc) "interleaving" were also examined (e.g., Figures 11D and 12D), and for an eclipsed structure, reasonable agreement between calculated and observed patterns was found (the most significant difference between Figure 12B and D is at $2\theta = 26.1°$—the 101 reflection in the primitive structure). Calculations of significantly staggered ($\phi > 10°$) interleaved structures of this type produced less satisfactory agreement. These results indicate that the [Ge(Pc)O]$_n$ diffraction data can also be analyzed in terms of the structural model shown in Figure 1, with a significant probability that, as in [Ga(Pc)F]$_n$ and presumably as a consequence of the larger interplanar spacing, the Pc rings are eclipsed rather than staggered. Data are set out in Table IV.

The powder diffraction data for [Sn(Pc)O]$_n$ could be best fit to a simple tetragonal cell (Figures 13B and 14B) with eclipsed rings. However, the agreement between calculated and observed intensities was not as close as might be expected (for example, the 001 reflection at $2\theta = 23.30$ appears to be anomalously weak), and furthermore, calculated interstack H–H distances were as short as 1.50 Å.[57b] Indeed, for this type of structure, it was not clear why the *a* dimension of the cell should be nearly 0.5 Å smaller than for the germanium analogue. A reasonable explanation for the discrepancies is a slight buckling of the phthalocyanine framework. This is a common porphyrin, phthalocyanine structural response to the incorporation of large metal ions[22,23b] and has been reported, in preliminary form, for Sn(Pc)Cl$_2$.[22b] Here, adjacent isoindoline planes are bent ±10.7° above or below the SnN_4 plane (I, where + indicates displacement above the plane of the page and – below the plane of the page). Theoretical powder patterns were next generated for crystal structures in which Sn(Pc)

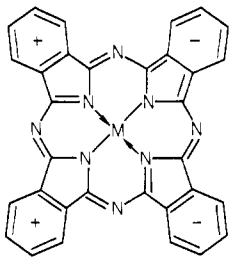

I

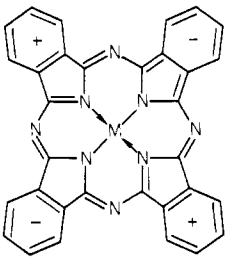

J

units were distorted as in I (10° buckling angles),[58] as in J (with 10° buckling angles),[59] and as in Figure 13C (10° buckling angles),[60] which is closely analogous to the molecular structure of Pb(Pc).[42b,61] Of these models, the second and third gave essentially equivalent and improved agreement with the experimental data, while the first model exhibited significant discrepancies in the $2\theta = 9.75°$ and 27–30° regions. The fit to the third model is shown in Figure 14C. Derived crystallographic parameters are set out in Table IV.

In principle it is possible to derive information on polymer crystallite dimensions from analysis of the diffraction line widths.[62] Although a complete discussion of this topic is reserved for a later contribution, a preliminary analysis of the present data has been carried out using the very sharp diffraction pattern of Ni(Pc) to obtain an approximate instrumental broadening factor. Using the simple Scherrer equation,[62,63] it was possible to estimate the mean crystallite dimension (L) in the various crystallographic directions. For $[Si(Pc)O]_n$, $[Ge(Pc)O]_n$, and $[Sn(Pc)O]_n$ we calculate $L > 200$ Å with no evidence for gross anisotropies in the different crystallite dimensions. These preliminary results are in accord with the molecular weight determinations. Further investigations are in progress.

(58) The best fit was for space group $P2_1/b$ with $\alpha = 12.81$ (5) Å, $b = 25.62$ (5) Å, $c = 3.82$ (2) Å, $\gamma = 90°$, $Z = 2$, $\psi = 28°$, and a calculated density of 1.71 g cm^{-3}.

(59) The best fit was for space group $P\bar{4}$, $a = 12.81$ (5) Å, $c = 3.82$ (2) Å, $Z = 1$, and a calculated density of 1.71 g cm^{-3}.

(60) Parameters are shown in Figure 13C.

(61) Here, eclipsed, saucer-shaped Pb(Pc) units stack in a monoclinic cell ($P2_1/b$) of dimensions $a = 25.48$ (8) Å, $b = 25.48$ (8) Å, $c = 3.73$ (1) Å, and $\gamma = 90°$.

(62) Klug, H. P.; Alexander, L. E. "X-ray Diffraction Procedures for Polycrystalline and Amorphous Materials"; Wiley-Interscience: New York, 1974; Chapter 9.

(63) This relationship assumes that noninstrumental broadening is due exclusively to crystallite size (as opposed to lattice strain, inhomogeneities, etc.). It is given by

$$L = K\lambda/(\beta \cos \theta)$$

where L is the mean dimensionality of the crystallites, K is an empirical constant (usually taken as 1.0), β is the breadth of the pure diffraction profile, and θ is the Bragg angle for the particular reflection.

Discussion

The principal objective of this investigation was to provide a chemical/spectroscopic/structural information base for studies of acceptor- and donor-doped electrically conductive polymers consisting of cofacially assembled group 4A metallophthalocyanines. It is seen that improved synthetic routes to these materials are now at hand and that the vibrational and optical spectra, prior to doping, are understandable in terms of simple mononuclear metallophthalocyanines. Molecular weight determinations by two different techniques establish these materials as polymers and suggest that, in the future, it should be possible to examine the physical properties of materials with systematically varied degrees of polymerization. The above results combined with the X-ray diffractometric analysis provide what may be the most accurate structural picture derivable for such materials in the absence of single crystals. These results strongly support the basic structural motif originally suggested by Kenney two decades ago and indicate that a means is truly available to vary the stacking architecture in a low-dimensional molecular/macromolecular material while keeping the structural and electronic characteristics of the molecular subunits nearly identical. With this information in hand, we explore in the accompanying contribution[14a] the chemical, structural, electrical, magnetic, and optical response of these systems to halogen dopants, which transform them from insulators into electrically conductive polymers.

Acknowledgment. This research was generously supported by the Office of Naval Research and by the NSF-MRL program through the Materials Research Center of Northwestern University (Grant DMR79-23573). We thank Professor J. B. Cohen and Dr. P. Georgopoulos for access to the X-ray diffraction equipment and for helpful advice concerning its use. We thank D. Keszler for helpful advice concerning the use of LAZY PULVERIX, and Professors V. W. Day, B. M. Foxman, and M. E. Kenney for helpful comments.

Registry No. $[Si(Pc)O]_n$, 39114-20-0; $[Ge(Pc)O]_n$, 55948-70-4; $[Sn(Pc)O]_n$, 57156-42-0; $Si(Pc)Cl_2$, 19333-10-9; $Ge(Pc)Cl_2$, 19566-97-3; $Sn(Pc)Cl_2$, 18253-54-8; $Si(Pc)(OH)_2$, 19333-15-4; $Si(Pc)(^{18}OH)_2$, 84647-97-2; $Si(Pc)(O^3H)_2$, 84647-98-3; $Ge(Pc)(OH)_2$, 16971-95-2; $Ge(Pc)(O^3H)_2$, 84647-99-4; $Sn(Pc)(OH)_2$, 12102-36-2; $Sn(Pc)(O^3H)_2$, 84648-00-0; 1,3-diiminoisoindoline, 3468-11-9.